A solar-powered hand-launchable UAV for low-altitude multi-day continuous flight

Philipp Oettershagen[1], Amir Melzer, Thomas Mantel, Konrad Rudin,
Rainer Lotz, Dieter Siebenmann, Stefan Leutenegger, Konstantinos Alexis and Roland Siegwart

***Abstract*— Abstract. Idea for this paper:**

- Conceptual design, realization/integration, development of onboard systems, flight testing and verification of conceptual/preliminary design =¿ Complete cycle including all steps can be shown here. - Demonstrations -¿ rather basic control approaches chosen, i.e. this platform will be the basis for further research in control, guidance & navigation, mapping and will go towards the applications of XXX - solar-powered, hand-launchable 5m-class Unmanned Aerial Vehicle with multi-day continuous flight capability combined with payload capacity for long-endurance SAR and inspection missions. Questions: - This paper = engineering paper, rest is then BASING upon this paper (use it as a ref). Is this OK? Is the chance that this will be accepted big enough? -¿ Yes, focus on "complete cycle" here, with more details in papers XXX to YYY

- We ware special : mission applications possible, long endurance, combination

I. INTRODUCTION

A. Introduction to solar-powered UAVs

When carefully designed, solar-electrically powered fixed-wing Unmanned Aerial Vehicles (UAVs) can exhibit significantly increased flight endurance over purely-electrically or even gas-powered aerial vehicles. Given certain environmental conditions and flight performance, a solar-powered UAV creates ´surplus energy´ when observed over a full day-night cycle, i.e. it will fully recharge its batteries during the day to continue flight through the night and potentially also the following day-night cycles. Long endurance - and especially this multi-day continuous flight capability often termed ´perpetual endurance´ - is of significant interest for large-scale mapping, observation or telecommunications relay applications as they occur in Search-And-Rescue (SAR) missions, industrial or agricultural inspection, meteorological surveys, border patrol and more [3].

Research in solar-powered UAVs of the High-Altitude Long Endurance (HALE) type has been going on since the 1990s [10]. Recently, interest in employing these large-scale UAVs (wing span above 20m) as ´atmospheric satellites´ - i.e. stationary/loitering platforms e.g. for telecommunications relay - has peaked [REF aquisitions]. Notable examples of this trend are Solara 50 [REF] and Zephyr[QinetiQ], the latter of which has already demonstrated a continuous flight of 11 days[REF QinetiQ]. In contrast, smaller scale solar-powered UAVs are mostly designed for Low-Altitude Long Endurance (LALE) applications. While they have to cope with the more challenging meteorological phenomenas of the lower atmosphere (clouds, rain, wind gusts or thermals), they generally have the advantage of lower complexity and cost, easier handling and generally faster response times through hand-launchability as required by First-Aid response teams in SAR scenarios[REF?]. However, research in small-scale solar UAVs targeting perpetual endurance has been relatively sparse, with most research focussing on conceptual design studies without extensive flight experience, e.g. [9]. However, in 2005, Cocconi's SoLong [2] performed a continuous 48 hours flight using solar power and thermal-updraft hunting. In addition, Noth [10] presents the conceptual design methods, realization and experimental flight results of the 3.2m wing span "SkySailor" airplane, which demonstrated a 27 hours solar-powered continuous flight without the use of thermals in 2008.

Fig. 1. The AtlantikSolar solar-powered UAV developed at ETH Zurich

B. Contributions of this paper

This paper aims to extend the work of [2], [10] by presenting AtlantikSolar, a solar-powered LALE-UAV with a wing span of 5.6m designed towards more robust multi-day operation capabilities while providing the option to use a visual&infrared sensor systems and on-board computation ressources developed at ETH Zurich. The contribution of the paper lies in presenting the complete development cycle from conceptual design to actual testing and missions, or more specifically

1) The application and extension of the conceptual design approach in [10], [7] towards more robust multi-day

All authors are part of the Autonomous Systems Lab, Swiss Federal Institute of Technology Zurich (ETH Zurich). Leonhardstrasse 21, 8092 Zurich, Switzerland.

[1] E-Mail:philipp.oettershagen@mavt.ethz.ch

*This work was supported by a number of project partners and generous individuals, see http://www.atlantiksolar.ethz.ch/

flight under sub-optimal meteorological conditions
2) The realization of the conceptual design results in the UAV hardware, i.e. structure, low-level electronics & avionics
3) The development of onboard EKF state estimation algorithms and PID with non-linear guidance flight control methods
4) The discussion of flight test results including long-endurance flight (up to 12hrs) and mapping results during examplary Search-And-Rescue missions.

II. CONCEPTUAL DESIGN

A. Methodology

The conceptual design methodology for solar-powered UAVs used in this paper was developed at ETH Zurich by [10], [7] and is briefly summarized below. To analyze flight performance and a potential perpetual flight capability, the energy input/output-balance needs to be modeled. The total required electrical power

$$P_{out,nom} = \frac{P_{level}}{\eta_{prop}} + P_{av} + P_{pld} \tag{1}$$

consists of the required electrical propulsion power for level-flight $\frac{P_{level}}{\eta_{prop}}$, where η_{prop} includes propeller, gearbox, motor, and motor-controller efficiency, and the necessary avionics and payload power P_{av} and P_{pld}. The aircraft is assumed to fly at the airspeed of minimum sink rate and thus minimum power consumption, i.e. its aerodynamic level-flight power is

$$P_{level} = \left(\frac{C_D}{C_L^{\frac{3}{2}}}\right)_{min} \sqrt{\frac{2(m_{tot}g)^3}{\rho(h)A_{wing}}}. \tag{2}$$

Here, $m_{tot} = m_{bat}+m_{struct}+m_{prop}+m_{sm}+m_{av}+m_{pld}$ is the total airplane mass, where structure, propulsion and solar module masses $m_{struct}, m_{prop}, m_{solar}$ are automatically sized according to [10], [7] and m_{av}, m_{pld} are given in table II-C. The local earth gravity is designated by g, A_{wing} is the wing area, and rho is air density. The airplane lift and drag coefficients C_L and C_D are retrieved from 2-D airfoil simulations using XFoil [4], with C_D being combined with parasitic drag from the airplane fuselage and stabilizers and the induced drag

$$C_{D,ind} = \frac{c_L^2}{\pi \cdot e_0 \cdot \lambda}. \tag{3}$$

Here, $e_0 \approx 0.92$ is the Oswald efficiency and λ is the wing aspect ratio. On the input side, the solar input power

$$P_{solar} = I \cdot A_{sm} \cdot \eta_{sm} \cdot \eta_{mppt} \tag{4}$$

considers the solar module area $A_{sm} = ff_{sm} \cdot A_{wing}$ with relative fill-factor ff_{sm}, module efficiency η_{sm}, and Maximum Power Point Tracker (MPPT) efficiency η_{mppt}. The solar radiation $I = I(\varphi, h, t)$ is assumed to be a function of the geographical latitude φ, the altitude h, and the current

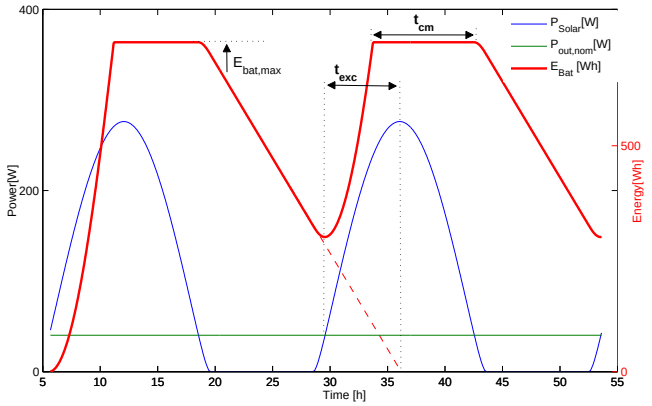

Fig. 2. Energetic simulation of a specific UAV configuration (Atlantik-Solar), showing input and output power, battery capacity, and performance metrics excess time t_{exc} and charge margin t_{cm} during a 2-day flight.

date and local time t, and is modeled as in [5]. The state equation can now be formulated in a simplified form as

$$\begin{aligned} \frac{dE_{bat}}{dt} &= P_{solar}(\varphi, h, t) - u - P_{av} - P_{pld}, \\ \frac{dh}{dt} &= \frac{\eta_{prop} \cdot u - P_{level}(h)}{m_{tot} g}. \end{aligned} \tag{5}$$

Here, u is the actual electrical power sent to the propulsion system. Simple forward integration of the state equation (5) gives the battery state of charge (SoC) over time and thus determines the perpetual flight capability.

For the design optimization, we assume that a solar-powered UAV configuration is designed for missions at and around a specific date of the year (DoY) and geographical latitude φ, and thus φ and DoY are fixed parameters. The three design parameters to be optimized are

- The wingspan b and wing aspect ratio λ, which specify wing geometry and thus influence the level-power in (2) and the solar input power in (4).
- The battery mass m_{bat} contained in m_{tot} in (2)

B. Extension of conceptual design optimization criteria

The conceptual design tool developed in [10], [7] has been extended in two ways: First, it now provides the capability to perform energetic simulations of multi-day solar-powered flight, whereas before only one day-night cycle was considered. Fig. XXX shows the results for incoming solar power P_{solar}, required power $P_{elec,tot}$, and remaining battery charge E_{bat} obtained for a two day/night cycle flight. Clearly, the initial charge condition E_{bat} at $t = t_{sunrise}$ for the second day is different than on the first day, which significantly reduces the required charge time until $E_{bat} = E_{bat,max} = m_{bat} \cdot e_{bat}$ and leads to increased charge margins with respect to the pure one day/night-cycle simulation.

Second, and more importantly, the optimization criteria are extended with respect to [10], [7] to achieve more robust multi-day flight. In general, a necessary and sufficient condition for perpetual flight is that the excess time $t_{exc} > 0$, i.e. that at $t = t_{eq}$ there exists remaining battery capacity to continue flight e.g. in case of cloud coverage in the morning. This is why[10], [7] focus on maximizing t_{exc}. However,

a large t_{exc} does not provide direct robustness against disturbances in P_{solar} during the charging process(e.g. due to clouds). In contrast, when optimizing purely for t_{exc}, the methodology in sec. II-A will select the largest battery size (due to the scaling of P_{level} with m_{bat}) which can still be fully charged unter optimal conditions, but every reduction in P_{solar} will directly decrease t_{exc} due to only partially charged batteries. We thus introduce the charge margin t_{cm} as the time margin between achieving the full charge $E_{bat} = E_{bat,max}$ and restart of the discharge in the evening. In case of decreased solar power income, $t_{cm} > 0$ will provide an additional margin before a decrease in excess time occurs.

The overall approach for increasing robustness with respect to local disturbances in the power income and output is thus to determine the lowest acceptable t_{exc} satisfying the UAV application requirements, and to then optimize the configuration for t_{cm}. The exact procedure applied here is:

- Choose the nominal operating latitude φ, the nominal Day-of-Operation DoY_{nom}, and the outermost days where perpetual UAV endurance is required $DoY_{min,max}$
- Obtain $t_{night,min}$ and $t_{night,max}$ for the range of $DoY_{min,nom,max}$ from [5].
- The required excess time $t_{exc,req}$ is now the sum of
  - $t_{exc,DoY} = t_{night,max} - t_{night,min}$
  - $t_{exc,clouds}$, to allow a margin for clouds in the morning or evening
  - $t_{exc,P_{level}}$, to allow a margin for increased power consumption e.g. caused by downdrafts or uncertainties in estimating P_{level}
- Perform the design analysis given the methodology in sec. II-A for $DoY(t_{night} = t_{night,min})$. Pre-select the subset $\mathcal{S}$ of configurations satisfying $t_{exc} > t_{exc,req}$.
- Within $\mathcal{S}$, choose the configuration $\mathcal{S}_i$ with the largest t_{cm}, taking into account UAV-specific further constraints on the design parameters b,$lambda$, or m_{bat}.

This conceptual design methodology is applied below. An alternative conceptual design approach utilizing a weighed version of t_{exc} and t_{cm} is proposed in [9].

C. Application of Conceptual Design methodology

AtlantikSolar is designed for a nominal operating latitude of $\varphi = 45N$. It shall provide perpetual endurance within a +/-2 month window around DoY_{nom}=June 21st (April 21st-August 21st). From [5], we find $t_{night,min} = 8.7h$ (June 21st), $t_{night,max} = 10.5h$(April 21st), and thus $t_{exc,DoY} = 1.80h$. We choose $t_{exc,clouds} = 3.0h$ to account for three hours of full cloud coverage either on the evening or the morning and choose $t_{exc,P_{level}} = 0.2 \cdot t_{night,max} = 2.1h$ to cover increased power consumption due to modelling errors, downdrafts or headwinds. Using $t_{exc,req} = t_{exc,DoY} + t_{exc,clouds} + t_{exc,P_{level}}$, we retrieve $t_{exc,req} = 6.9h$ as the minimum required excess time for robust perpetual-flight at the given dates and locations.

The design methodology tool of section II-A is now applied assuming the fixed component performance parameters

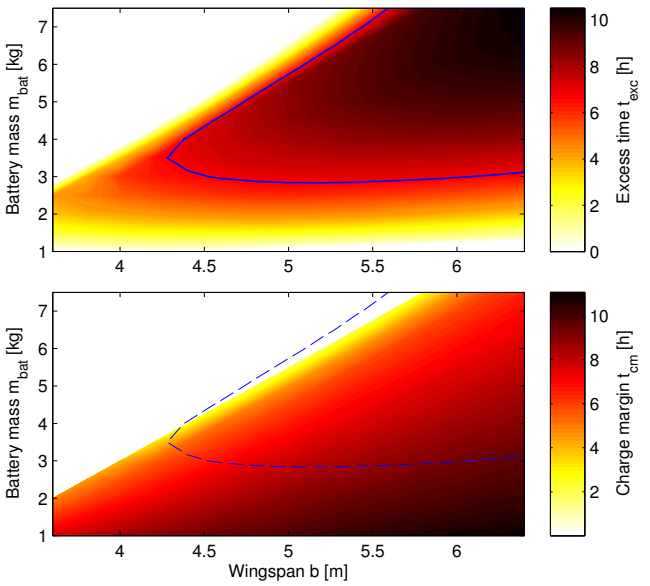

Fig. 3. Excess time t_{exc} (top) and charge margin t_{cm} (bottom) vs. optimization parameters wingspan b and m_{bat}, all at $\lambda = 18.5$. The configuration subset $\mathcal{S}$ satisfying $t_{exc} > t_{exc,req}$ under our design requirements lies inside the blue contour line.

in Tab. II-C. Fig. 3 shows the resulting plot for t_{exc} versus the optimization variables wing span b, battery mass m_{bat} and aspect ratio $\lambda = 18.5$. The subset $\mathcal{S}$ of configurations satisfying $t_{exc} > t_{exc,req}$ is the region within the blue contour-line. The optimum clearly occurs at large wing spans, however, considering an external size constraint (each of the three wing pieces of AtlantikSolar shall be $< 2m$ in wing span to allow proper handling and transport), we choose $b = 5.6m$. The aspect ratio $\lambda = 18.5$ is found to provide an optimum in t_{exc}, and also allows to seamlessly integrate the solar cells (see section XXX) inside the wing chord. The last design choice is now m_{bat}, for which we seek to optimize t_{cm} within the previously selected set $\mathcal{S}_1 = (\mathcal{S}|b = 5.6m, \lambda = 18.5)$. As visible in Fig. 3, $m_{bat} = 3.0...7.5kg$ lie within $\mathcal{S}_1$. We choose $m_{bat} = 3.5kg$ to optimize t_{cm} and due to practical battery sizing constraints described in sec XXX. The selected configuration thus has an overall estimated mass of $m_{tot} = 7.22kg$ and yields an estimated $t_{exc} = 7.89h$ and $t_{cm} = 8.38h$ for the nominal operating date and latitude.

TABLE I
FIXED PARAMETERS FOR THE CONCEPTUAL DESIGN

Parameter	Value	Description
eta_{sm}	0.20	Solar module efficiency
eta_{MPPT}	0.97	MPPT efficiency
eta_{prop}	0.58	Propulsion system effiency
e_{bat}	874800W/kg	Battery specific energy
ff_{sm}	0.94	Solar module fill factor
k_{sm}	0.59kg/m	Solar module areal density
m_{av}	0.6kg	Avionics mass (including all cabling)
m_{pld}	0.1kg	Payload mass
P_{av}	4.5W	Avionics power consumption
P_{pld}	0.0W	Payload power consumption

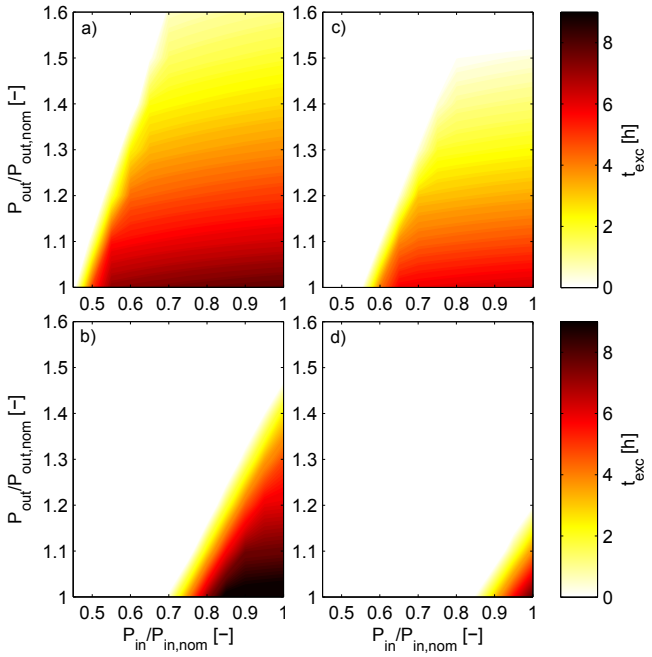

Fig. 4. Excess time t_{exc} under disturbed power input and output for the developed $b = 5.6m$, $\lambda = 18.5$ configuration: a) m_{bat}=3.5kg on June 21st b) $m_{bat} = 6.0kg$ on June 21st c) m_{bat}=3.5kg on April 21st d) $m_{bat} = 6.0kg$ on April 21st

D. Robustness analysis

To verify the multi-day flight robustness of the developed UAV configuration, we analyze its performance considering a set of local disturbances in UAV power input and output, namely

- The disturbed solar power income $P_{in,dist}$, as caused by various forms of clouds or fog. Lacking knowledge of the exact spatial and temporal cloud distribution, we'll assume the simple scaling

$$P_{in}(t) = P_{in,nom}(t) \cdot k_{CCF}.$$

  Here, $k_{CCF} = [0, 1]$ represents the current cloud cover factor [6], i.e. the clearness of the atmosphere.
- The disturbed electrical power output $P_{out,dist}$. Wind downdrafts, head wind, or wind gusts may require increased propulsion or actuation power. Again, we'll assume the scaling

$$P_{out}(t) = P_{out,nom}(t) \cdot k_{OPF},$$

  with OPF representing the Output Power Factor.

Fig. 4 shows the remaining excess time with respect to these disturbances. The UAV configuration developed in section II-C (with $m_{bat} = 3.5kg$) still provides perpetual endurance with less than 50% of the solar power income or if more than 60% surplus power are required e.g. to compensate for downdrafts on June 21st (Fig.4a). In contrast, a configuation purely optimized towards excess time with $m_{bat} = 6.0kg$ will yield a higher maximum t_{exc} of 9.5h, however, the robustness with respect to clouds or higher required level power is greatly decreased (Fig.4b). On April 21st, the UAV configuration of section II-C still provides solid robustness, which verifies the +/-2month perpetual endurance requirement (Fig.4c). In contrast, the $m_{bat} = 6.0kg$ configuratoin can not provide reliable perpetual endurance anymore (Fig.4d). This analysis verifies the advantages of the extended optimization criteria for achieving maximum robustness in perpetual endurance.

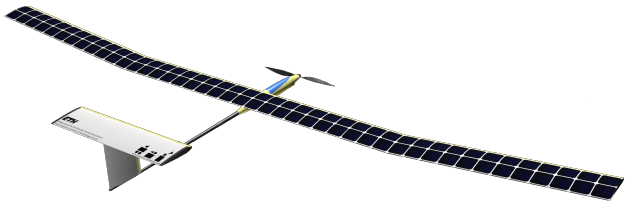

Fig. 5. The AtlantikSolar UAV features a conventional T-tail configuration with 1 motor, two ailerons, an all-moving elevator and a rudder for actuation.

TABLE II
ATLANTIKSOLAR DESIGN CHARACTERISTICS

Wing span	5.65m
Wing chord	0.305m
Length	
Height	
Mass	7.36kg
Battery mass	3.52kg
Wing loading	$4.28^{\mathrm{kg}}/_{\mathrm{m}^2}$
Stall speed	$8.1^{\mathrm{m}}/_{\mathrm{s}}$ TBD

III. DETAILED DESIGN AND REALIZATION

AtlantikSolar (Figs. 1 and 5) is a solar-powered Low-Altitude Long-Endurance(LALE) Unmanned Aerial Vehicle designed for perpetual flight at $\varphi = 45$ geographical latitude from April 21st to August 21st. It was designed and built at ETH Zurich as a lightweight high aspect ratio airplane to achieve minimum sink rate. Although its design is mostly dictated by the requirement for low power consumption, it does provide the option to use visual&infrared sensor systems and on-board computation ressources in an autonomous operation mode for use in search and rescue or industrial inspection applications. The airplane design is summarized in table III. Figure 7 presents an overview over the aircraft components topology.

A. UAV Platform Design

1) Airframe and hardware: The structure of AtlantikSolar is built in a traditional rib-spar construction method. The wing (Fig. 6) consists of an inner cylindrical carbon-fibre spar to resist torsional wing loads. Four carbon-fibre belts of trapezoidal and laterally-varying cross-section are located around the spar to optimally resist bending loads and to provide maximum wing stiffness to protect the solar cells on the wings. Equally-spaced balsa-wood ribs and the kevlar-reinforced wing leading edge provide structural support for the non-load-carrying outer wing surface. The horizontal and vertical tail planes are constructed in a similar fashion.

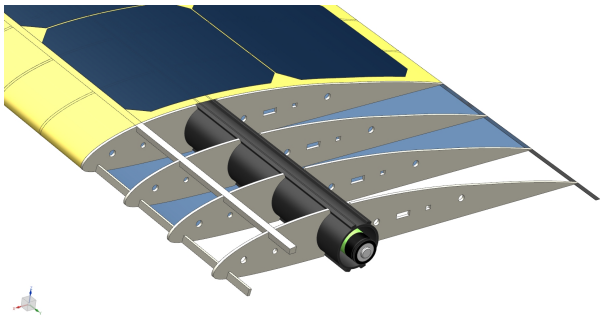

Fig. 6. AtlantikSolar's wing structure, integrated batteries and solar cells.

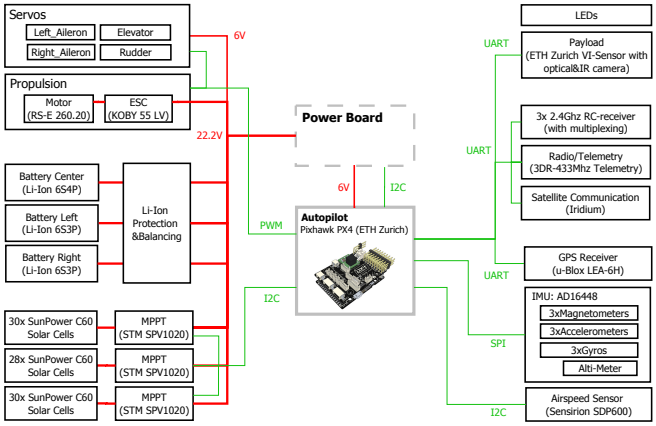

Fig. 7. AtlantikSolar system overview. For clarity, voltage lines from the autopilot to connected devices (5.0V and 3.3V) are omitted.

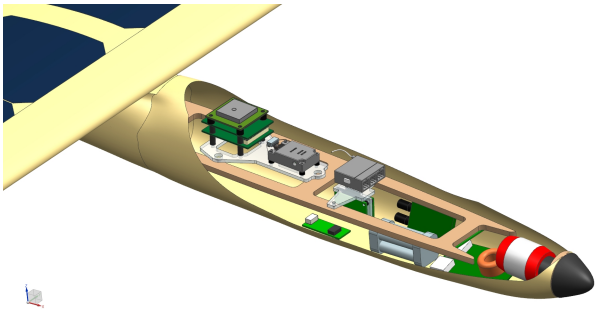

Fig. 8. Avionics components and their placement inside AtlantikSolar.

The cylindrical wing spar contains a total of 60 cylindrical Lithium-Ion battery cells to optimally distribute the battery mass in a "span loader" concept. An additional 12 batteries can be added inside the outer wings to optimize the aircraft for a specific application. The Li-Ion cells are Panasonic NCR18650b high energy density (243Wh/kg) industrial cells.They are connected in a 6S (22.2V) configuration and provide $E_{bat,max} = 850Wh$ at $m_{bat} = 3.5kg$. The solar modules are seamlessly embedded into the upper wing surface to avoid premature flow separation. They feature a total of 88 SunPower C60 cells with a measured module-level efficiency of $\eta_{sm} = 0.20$, an areal density of $k_{sm} = 590g/m^2$ and a maximum power output of 275W at $\varphi = 45$ on June21st. Modules featuring SunPower E60 cells with a verified module-level efficiency of $eta_sm = 0.23$ are currently being integrated.

The propulsion system features a foldable carbon-fibre propeller with $D = 66cm$ and 60cm pitch that was specifically developed to achieve $\eta_{propeller} = 82\%$ at the nominal operating point of $F_{propeller} = 2.4N$ at $v = 8.5$m/s. The propeller is driven by a 5:1 reduction-ratio planetary gearbox, a RS-E Strecker 260.20 brushless DC motor with $k_V = 570RPM/V$ and a Kontronik Koby 55 LV motor controller. The propulsion system delivers a maximum electrical power of $P_{prop,max} = 450W$. The actuation system consists of four Volz DA-15N servos that drive the two ailerons, the all-moving elevator and the rudder. To guarantee reliable multi-day flight, the Volz actuators were successfully bench-tested throughout a simulated continuous 30-day flight [1].

2) Avionics: The AtlantikSolar avionics topology is shown in Fig. 7 and an integration snapshot is presented in Fig. 8. Multiple sensors are centered around a Pixhawk PX4 Autopilot - an open source and open hardware project initiated at ETH Zurich - with a Cortex M4F microprocessor running at 168Mhz and featuring 192kB RAM. For state estimation (section XXX), an ADIS 16448 10-axis Inertial Measurement Unit (IMU), a u-Blox LEA-6H GPS receiver, and a Sensirion SDP600 differential pressure (i.e. airspeed) sensor are used. The SDP600 airspeed sensor has been chosen due to its low relative error of less than 5% at airspeeds of 8m/s, which is necessary to closely control the airspeed to the airspeed with minimum required power P_{out}. Commands are received through a 433Mhz telemetry link for medium ranges, or through a long-range IRIDIUM-based satellite communication link that also serves as a backup in case of primary telemetry link failure. The airplane implements a fully manual RC-command fallback mode in case of a severe autopilot failure. Night operations are possible due to four on-board high-power LEDs.

3) Payload: - VI Sensor [ref to VI-sensor paper; ref to Leutenegger thesis?] - 5 sentences + 1 picture

B. State Estimation and Control Design

1) State estimation: The on-board state estimator based on extended Kalman filter (EKF) offers a robust estimation solution and can cope with prolonged GPS outage scenarios. It is implemented and optimized in order to grant full functionality on the on-board computation unit. Successive estimations of the position, velocity, orientation (attitude and heading), QFF, gyroscopes biases, accelerometers biases and the wind vector are rendered by the state estimator. Moreover additional estimations as the sideslip angle and the angle of attack (AoA) can be derived. A set of on-board sensors as inertial measurement unit (MEMS based), dynamic and static pressure sensors, magnetic compass and GPS receiver deliver the necessary data for the state estimator.A detailed description of the state estimator can be found in [8].

2) System Identification: - System Identification & Modelling

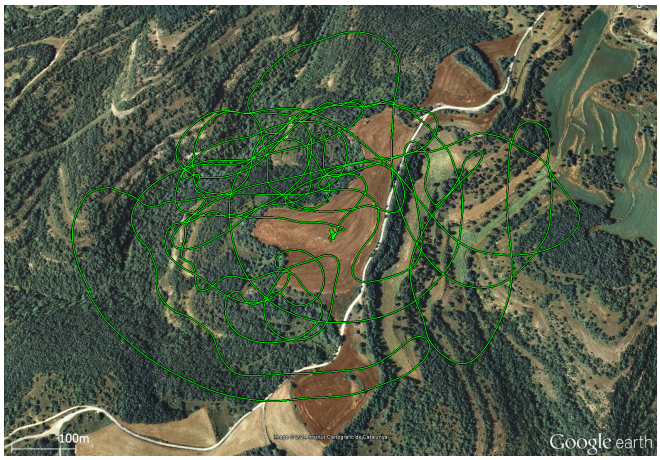

Fig. 9. Overhead trajectories plot of the on-board position state estimation (green) and the GPS (black).

3) Control: - Control using PID, outer loops TECS & L1 (Ref to OMLAS MED paper, also saying that there is future technologies which are being developed). - Full pre-flight verification in HIL

C. Preliminary Results

- control: - SE&Control: PID performance over various trim points. PID computational requirements (low!) - state estimation - solar system functioning - power efficiency curves. P_level from Test flights. - potentially comparison to conceptual design - power (why not optimal: e.g. because optimal CD/CL$\hat{1}$.5 assumed, but this has a) to be met in average and b) even then fluctuations as seen in flight tests are on the order of 2-3 degrees in AOA or +/- 1m/s, so this will never be met perfectly. - actual mass vs. mass models?

IV. EXPERIMENTAL RESULTS

- mention Total flight hours, total flights. Mention that 2 AtlantikSolars have already been built & flown. Range of weather conditions?

A. Subsystem level results

- power efficiency curves. P_level from Test flights. - solar power system and rechargin of batteries? - control results? [if not already shown before]. - control: - SE&Control: PID performance over various trim points. PID computational requirements (low!)

B. Continuous 12hour Flight

C. Mapping Flights in Search and Rescue scenarios

- mapping missions in ICARUS. - REF to Separate paper??? Yes, but only once both are accepted. - some cool pics/reconstructed maps

V. CONCLUSIONS

Mention: - Main lessons learned / summarize main points of paper - Future work

CHECK AT END: - all references (especially: urls, capitalization)

APPENDIX

Appendixes should appear before the acknowledgment.

ACKNOWLEDGMENT

The preferred spelling of the word acknowledgment in America is without an e after the g. Avoid the stilted expression, One of us (R. B. G.) thanks . . . Instead, try R. B. G. thanks. Put sponsor acknowledgments in the unnumbered footnote on the first page.

REFERENCES

[1] Master's thesis.

[2] Alan Cocconi. Ac propulsion's solar electric powered solong uav. Technical report, AC Propulsion, 2005. Retrieved from {http://www.tu.no/migrationcatalog/2005/07/24/solong-info/binary/SoLonginfo}.

[3] N.J. Colella and G.S. Wenneker. Pathfinder: Developing a solar rechargeable aircraft. *IEEE Potentials*, 15(1):18–23, 1996.

[4] M. Drela. Xfoil 6.9 user primer. Technical report, MIT Aero&Astro, 2001. Retrieved from {http://web.mit.edu/drela/Public/web/xfoil/xfoil_doc.txt}.

[5] John A. Duffie and William A. Beckman. *Solar Engineering of Thermal Processes*. Wiley, 3rd edition, 2006.

[6] K. Kimura and D.G. Stephenson. Solar radiation on cloudy days. Technical report, National Research Council of Canada, 1969. Retrieved from {http://web.mit.edu/parmstr/Public/NRCan/rp418.pdf}.

[7] Stefan Leutenegger and Mathieu Jabas. Solar airplane conceptual design and performance estimation. *Journal of Intelligent Robot Systems*, 61:545–561, 2010.

[8] Stefan Leutenegger, Amir Melzer, Kostas Alexis, and Roland Siegwart. Robust state estimation for small unmanned airplanes. In *IEEE Multiconference on Systems and Control*.

[9] Scott Morton, Luke Scharber, and Nikalaos Papanikolopoulos. Solar powered unmanned aerial vehicle for continuous flight: Conceptual overview and optimization. In *IEEE International Conference on Robotics and Automation (ICRA)*.

[10] A. Noth. *Design of Solar Powered Airplanes for Continuous Flight*. PhD thesis, ETH Zurich, 2008.